



# Halogen (F, Cl, Br, I) behaviour in subducting slabs: A study of lawsonite blueschists in western Turkey



Lilianne Pagé<sup>a,\*</sup>, Keiko Hattori<sup>a</sup>, Jan C.M. de Hoog<sup>b</sup>, Aral I. Okay<sup>c</sup>

<sup>a</sup> Department of Earth and Environmental Sciences, University of Ottawa, Ottawa K1N 6N5, Canada

<sup>b</sup> School of Geosciences, University of Edinburgh, Edinburgh EH93JW, UK

<sup>c</sup> Department of Geology, Istanbul Technical University, Istanbul 34469, Turkey

## ARTICLE INFO

### Article history:

Received 12 November 2015

Received in revised form 12 February 2016

Accepted 27 February 2016

Available online xxx

Editor: B. Marty

### Keywords:

subduction

halogens

fluorine

lawsonite

phengite

deep mantle

## ABSTRACT

We examined the F, Cl, Br and I abundance of minimally retrogressed lawsonite blueschists from the Tavsanli Zone in northwest Turkey to evaluate the behaviour of halogens in subduction zones, and to determine the role coexisting high pressure minerals may play in transporting the halogens to the Earth's mantle. The blueschists contain sodic amphibole and lawsonite, with variable amounts of phengite and chlorite, and minor apatite. A positive correlation between Cl, Br and I contents in bulk rocks suggests their overall coherent behaviour in subduction zones, although high ratios of I/Cl and Br/Cl compared to altered oceanic crust indicate that Cl is preferentially lost relative to Br and I before or during blueschist metamorphism. Iodine and F are enriched relative to altered oceanic crust, suggesting incorporation from marine sediments. *In situ* analyses of minerals in thin sections reveal F preferentially concentrates in apatite (avg. 3.13 wt%), over phengite (482 ppm), lawsonite (avg. 413 ppm) and Na-amphibole (257 ppm). Chlorine also preferentially resides in apatite (138 ppm), followed by equal partitioning between phengite (59 ppm) and Na-amphibole (56 ppm), and lower concentrations in lawsonite (27 ppm). Upon apatite decomposition at a depth of ~200 km, F may redistribute into lawsonite and phengite in slabs, whilst Cl is likely expelled to the overlying mantle wedge. Given the stability of lawsonite and phengite to a depth of 280–300 km in cold subduction zones, they may transport F beyond subarc depths, contributing to the high F in magmas derived from the deep mantle.

© 2016 Elsevier B.V. All rights reserved.

## 1. Introduction

Halogens are predominantly concentrated in the Earth's surface reservoirs, including seawater and sediments. Their concentrations are low in the primitive mantle, with current estimates of 18 ppm F, 1.4 ppm Cl, 0.0036 ppm Br and 0.001 ppm I (Lyubetskaya and Korenaga, 2007). As halogens are not compatible with mantle minerals, they are preferentially removed from the mantle during partial melting, and as such their concentrations are even lower in the depleted MORB mantle (DMM). Despite having low concentrations in the mantle, halogens are abundant in mantle-derived magmas, and are continuously discharged from volcanoes of a variety of settings. For example, F and Cl are the most abundant constituents of volcanic gases discharged from arc volcanoes after H<sub>2</sub>O, CO<sub>2</sub> and S species (Symonds et al., 1994). The key mechanism responsible for volcanic outputs is the recycling of elements from surface reservoirs to the mantle through sub-

duction. Many studies have primarily focused on Cl in subduction zones, using it as a proxy for the other halogens (e.g. Scambelluri et al., 2004; Marschall et al., 2009).

During subduction, aqueous fluids released from the slab move upward to the overlying mantle wedge, which leads to partial melting of the interior of the hot mantle wedge for arc magmatism. The depth of fluid release is related to the geothermal gradient of the subduction zone and the stability of hydrous minerals. As halogens are soluble in aqueous fluids, their behaviour is expected to follow that of water, but the stability of hydrous minerals differs widely, and hydrous minerals have varying ability to accommodate fluid-mobile elements, including halogens. Therefore, the composition of fluids released from slabs is likely to change with increasing depth. Furthermore, some hydrous minerals, such as serpentine (~13 wt% H<sub>2</sub>O), lawsonite (~ 11 wt% H<sub>2</sub>O) and phengite (~4 wt% H<sub>2</sub>O), are stable to depths of 200–300 km in cold subduction zones (Schmidt and Poli, 1998), far beyond the depths beneath arcs. This suggests that these minerals are able to transport not only water, but also fluid-mobile elements, to the deeper mantle.

\* Corresponding author.

E-mail address: lpage097@uottawa.ca (L. Pagé).

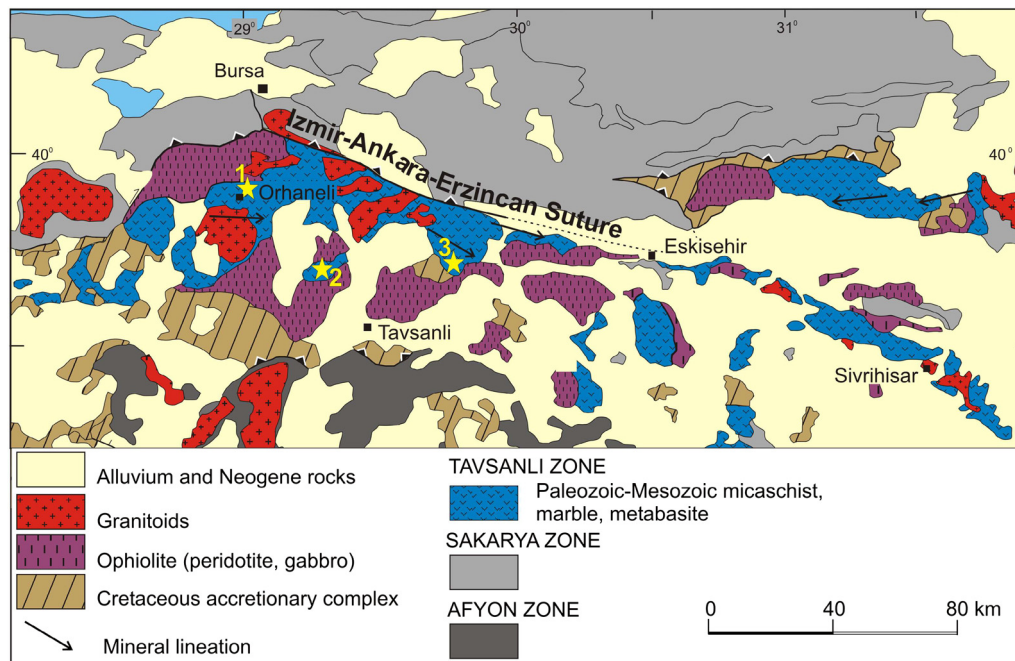


**Fig. 1.** Simplified geological map of the Tavsanlı Zone in northwestern Turkey (modified from Okay and Whitney, 2010). Sample outcrop locations are numbered and marked with stars.

Recent work has documented the importance of serpentinite in the transport and fractionation of the halogens in subduction zones (e.g. John et al., 2011; Kendrick et al., 2013), with their findings suggesting Br and I are preferentially released relative to Cl and F during serpentine phase transition and decomposition. However, there are few studies documenting the abundance of halogens in other hydrous minerals. This paper reports the abundance of halogens in lawsonite-bearing blueschists from the Tavsanlı Zone in northwestern Turkey using a variety of analytical techniques, and discusses the behaviour of halogens, particularly F, in subduction zones and the implications for global halogen recycling.

## 2. Geological setting

Turkey is comprised of several continental fragments that assembled during the Tertiary collision of Laurasia and Gondwana. In western Turkey, the İzmir–Ankara–Erzincan suture marks the collision of the southern and northern terranes. Prior to the collision, the margin of the southern continent, the Anatolide–Tauride Block, was subducted to a depth of 80 km by 80 Ma in an intra-oceanic subduction zone and was metamorphosed in blueschist facies (Sherlock et al., 1999; Okay and Whitney, 2010). The resulting blueschist belt, known as the Tavsanlı Zone, is exposed immediately south of the suture (Fig. 1). It is primarily comprised of Paleozoic–Mesozoic metabasites and metasedimentary rocks representing the subducted continental margin, in addition to tectonically overlying oceanic accretionary complex and peridotite. The east–west trending Tavsanlı Zone is 50–60 km wide and approximately 250 km long (Okay and Whitney, 2010). It is one of the most extensive and well-preserved blueschist belts in the world with little retrogression (Okay, 1980).

In the western part of the Tavsanlı Zone, the Orhaneli Group blueschists are divided into three units. The base is the quartz–mica–pelitic schists of the Kocasu Formation (Okay, 2002), which gradually changes to the overlying İnönü Marble. The mica schist consists of quartz, phengite, jadeite, chloritoid, Na-amphibole, lawsonite, and chlorite. The assemblage constrains the peak metamorphic conditions to  $24 \pm 3$  kbar and  $430 \pm 30$  °C, corresponding to a low geotherm of 5 °C/km (Okay, 2002). The uppermost

**Table 1**

Summary of sample mineralogy of Tavsanlı Zone blueschists in northwest Turkey.

Outcrop No. in Fig. 1	Sample ID	Mineralogy	
		Major	Minor
1	TUR12	Lws, Na-Amp, Chl, Jd, Ttn	Qtz, Ap, Ep
	TUR14	Lws, Na-Amp, Ph, Chl	Qtz, Ttn, Rt, Ap
2	TUR23	Lws, Chl, Ph, Ttn	Na-Amp, Ap, Py
3	TUR30	Lws, Na-Amp, Ph, Qtz, Chl	Ap, Ttn, Rt
	TUR31	Lws, Chl, Ph, Qtz	Ap, Ttn, Ab
	TUR32	Lws, Na-Amp, Qtz, Ab	Chl, Ttn, Ap
	TUR33	Lws, Na-Amp, Ph, Ap, Ttn	Fe-oxides, Chl

unit, the Devlez Formation, is composed of metabasite (>80 vol%) with minor metasedimentary rocks metamorphosed under similar blueschist facies conditions (Okay, 1980). The metabasites contain euhedral lawsonite laths in a matrix of foliated sodic amphibole with variable amounts of phengite and chlorite. Rb–Sr phengite ages of  $78.5\text{--}79.7 \pm 1.6$  Ma likely reflect the age of metamorphism in the region (Sherlock et al., 1999). These metabasites are the focus of this study.

## 3. Samples

Lawsonite-rich metabasites were collected from three outcrops of the western Tavsanlı Zone (Fig. 1). All samples contain idioblastic lawsonite laths (< few mm in length) with varying abundance of blue amphibole (Table 1). Samples are characterized by prograde mineral assemblages with very little retrograde products (e.g. no secondary calcic amphibole, and only minor epidote and albite).

Samples TUR12 and TUR14 are blueschists collected in the Orhaneli region, near the town of Deliballar (Okay and Whitney, 2010). TUR12 contains an intergrowth of prismatic lawsonite (<0.5 mm) and Na-amphibole grains (<0.5 mm), with minor chlorite (Fig. 2A). Lawsonite contains inclusions of quartz, Na-amphibole and titanite. There are interstitial quartz, apatite, Na–Ca pyroxene and minor epidote throughout the sample. Large (up to 4 mm) euhedral lawsonite of TUR14 are highly fractured and contain inclusions of Na-amphibole and minor quartz. They are set in

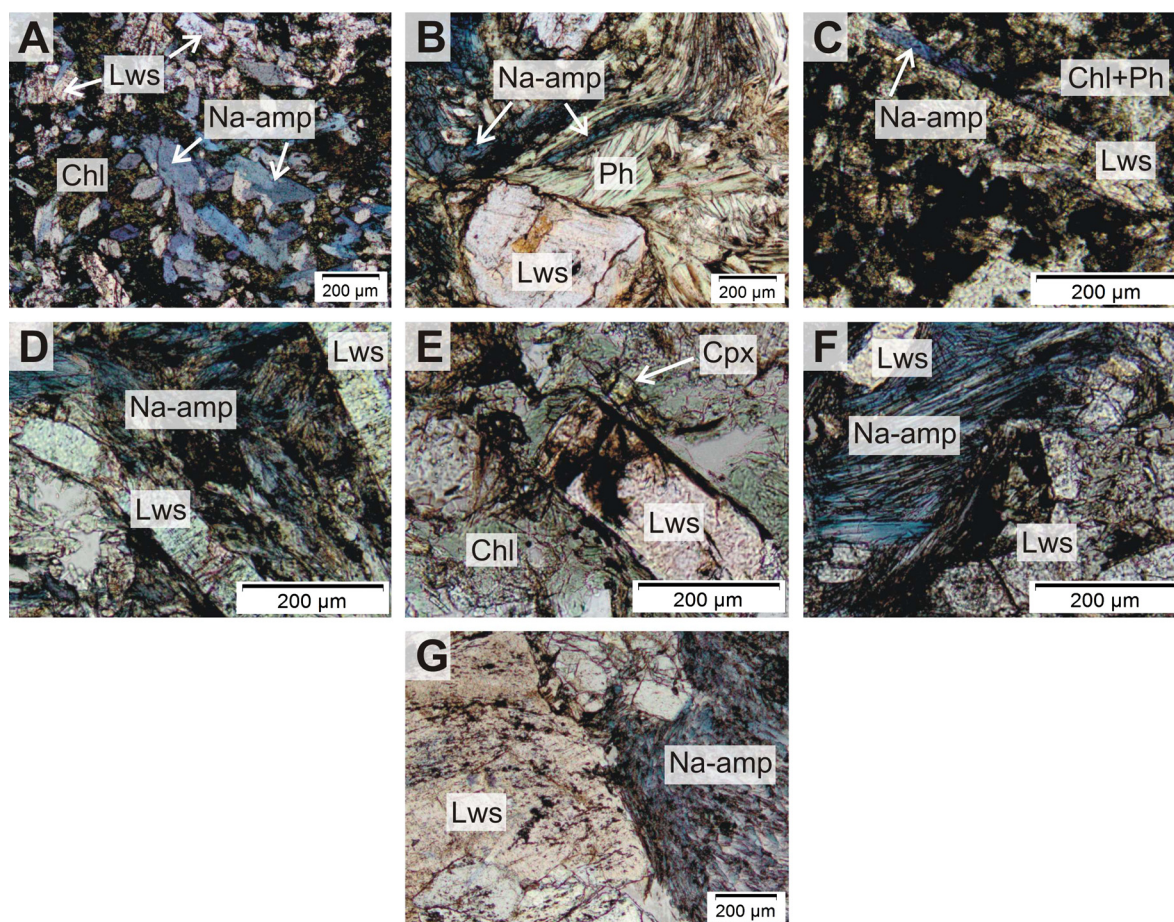


**Fig. 2.** Photomicrographs of lawsonite blueschist samples from the Tavsanlı Zone, northwest Turkey. (A) TUR12, (B) TUR14, (C) TUR23, (D) TUR30, (E) TUR31, (F) TUR32 and (G) TUR33. Chl: chlorite, Cpx: clinopyroxene, Lws: lawsonite, Na-amp: Na-amphibole, Ph: phengite. (For interpretation of the references to colour in this figure, the reader is referred to the web version of this article.)

a matrix of fibrous Na-amphibole prisms (and some larger grains up to 0.5 mm), in addition to fibrous chlorite and minor rutile. Phengite grains are larger than in other samples (up to 0.3 mm), and are often found in clusters (Fig. 2B). Blueschists from this region have been previously described by Okay (2002).

One sample (TUR23) was collected from a blueschist outcrop near Harmancik (southeast of Orhaneli). It contains clusters of idiomorphic lawsonite laths (~1 mm length) along with minor Na-amphibole needles (<0.2 mm) and minor titanite set in fine-grained aggregates of phengite and chlorite (Fig. 2C). The surrounding dark matrix is composed of fine-grained actinolite, chlorite, titanite, apatite and pyrite.

The remaining samples (TUR30, 31, 32, 33) were collected from the Devlez Formation near the village of Ketenlik, farther east along the Tavsanlı Zone (Fig. 1). Sample TUR30 is characterized by elongated lawsonite laths surrounded by Na-amphibole, phengite, quartz, minor apatite and minor titanite (Fig. 2D). The lawsonite laths of TUR31 vary in size (up to 1 mm) and contain inclusions of quartz and titanite. They are surrounded by green Na-amphibole, chlorite, interstitial quartz and disseminated albite and phengite (Fig. 2E). Wide (up to 5 mm) quartz veins are also present in the sample. TUR32 shows foliation defined by fibrous Na-amphibole and lawsonite laths (Fig. 2F). Na-amphibole is compositionally zoned with Al-rich cores and Fe-rich rims. There is also minor chlorite, quartz and titanite throughout the sample. Generally, TUR32 is more fine-grained than the other three samples from this area. TUR33 contains veins composed of large lawsonite laths (up to 5 mm), which are fractured and contain inclusions of Na-amphibole, apatite and magnetite, similar to those of

TUR14. Lawsonite is surrounded by a matrix of fine-grained fibrous Na-amphibole, iron oxides, apatite, titanite, phengite and minor chlorite (Fig. 2G). Some phengite forms aggregates up to 0.5 mm. Blueschists from this outcrop have been previously described by Okay (1980) and sampling locations are described in the field trip guidebook by Okay and Whitney (2010).

#### 4. Analytical methods

##### 4.1. Bulk-rock chemistry

Bulk rock major and minor element composition was determined by ALS Global (North Vancouver, Canada) using X-ray fluorescence (XRF) after fusion of rock powder with 50/50  $\text{Li}_2\text{B}_4\text{O}_7/\text{LiBO}_2$ , and trace element composition was determined at the same facility by ICP-MS following digestion of rock powder by concentrated  $\text{HF-HNO}_3\text{-HClO}_4\text{-HCl}$ .

##### 4.2. Halogen extraction: pyrohydrolysis + IC/ICP-MS

Amphibole-rich and lawsonite-rich fractions were separated from four samples (TUR14, 30, 32, 33) by hand under a binocular microscope. A phengite-rich fraction was also collected from TUR14. The remaining samples were too fine-grained for separation. Halogens were extracted from the mineral-rich fractions and bulk rock samples using a modified pyrohydrolysis technique after Muramatsu et al. (2007) and references therein. Method details are in Appendix A.

Analysis for F and Cl was carried out at the University of Ottawa using a Dionex Model 2100 Ion Chromatograph equipped with

KOH eluent generator. Instrumental detection limits ( $3\sigma$ ) for F and Cl were 0.017 ppm and 0.034 ppm in solution, respectively. Analysis for Br ( $^{79}\text{Br}$ ) and I ( $^{127}\text{I}$ ) was carried out at the University of Ottawa using an Agilent 7700 ICP mass spectrometer. Instrumental detection limits ( $3\sigma$ ) for Br and I were 0.022 and 0.041 ppb, respectively. Standard deviations ( $1\sigma$ ) for duplicate or triplicate analyses of samples are in the range 0.3–15% for F, 1.7–36% for Cl, 2.3–25% for Br, and 2.0–29% for I. Accuracy of the pyrohydrolysis technique is based on the analysis of four international reference materials (BCR-2, JB-1, JB-3 and MRG-1). Percent yield ranges from 76 to 93% for F, from 85 to 106% for Cl, from 66 to 111% for Br, and from 110 to 156% for I (refer to Table S1 in supplementary files for details).

### 4.3. Mineral chemistry

#### 4.3.1. Electron microprobe analysis (EPMA)

Na-amphibole, lawsonite and phengite were analyzed for Si, Ti, Al, Mg, Fe, Ca, Na, K, Mn, Cr and Ni at the University of Ottawa with a JEOL 8230 electron microprobe using a wavelength dispersive spectrometer. A 5  $\mu\text{m}$  diameter 20 nA beam accelerated to 20 kV was used. Peak counting times were 10 s per element for the  $K\alpha$  lines of Fe, Mn, Cr and Si, 20 s for K, Ca, P, Al, Ti, Na and Mg, and 50 s for Ni. Instrument calibration used sanidine (Si, Al, K), diopside (Ca, Mg), albite (Na), hematite (Fe), tephroite (Mn), San Carlos olivine (Ni), rutile (Ti), chromite (Cr) and apatite (P).

Mineral formulae of Na-amphibole grains were calculated using 23(O), and ferric and ferrous iron contents were determined on the basis of stoichiometric composition after normalizing to 8 Si atoms. For lawsonite, all iron was assumed to be  $\text{Fe}^{3+}$ , and mineral formulae were determined using 8(O). Mineral formulae of phengite and the amount of  $\text{Fe}^{3+}$  were calculated based on stoichiometric composition and charge balance using 11(O).

The analytical conditions for apatite were 10 kV accelerating voltage, 4 nA beam current, and 10  $\mu\text{m}$  diameter beam size as recommended by Goldoff et al. (2012) for optimal analysis of fluor-chlorapatites. Each grain was analyzed in 1–3 spot(s), depending on grain size. Peak counting times were 10 s per element for Si ( $K\alpha$ ), Fe ( $K\alpha$ ), Mg ( $K\alpha$ ), K ( $K\alpha$ ), S ( $K\alpha$ ), Ce ( $L\alpha$ ), La ( $L\alpha$ ) and As ( $L\alpha$ ), 20 s for Al ( $K\alpha$ ), Ca ( $K\alpha$ ), Na ( $K\alpha$ ), P ( $K\alpha$ ), Sr ( $L\alpha$ ) and Cl ( $K\alpha$ ), and 50 s for F ( $L\alpha$ ). Instrument calibration used sanidine (Si, Al, K), hematite (Fe), diopside (Mg), apatite (Ca, P, F), albite (Na), celestine (S, Sr),  $\text{CePO}_4$  (Ce),  $\text{LaPO}_4$  (La), and GaAs (As). The apatite standard contains 3.53 wt% F. An LDE1 diffraction crystal was used to enhance the count of F. Apatite mineral formulae were calculated based on normalizing to 13 (O, OH, F, Cl).

#### 4.3.2. Ion microprobe analyses (SIMS)

Grains for *in situ* analyses were selected from EPMA-analyzed samples. Grains were cored from polished thin sections using a diamond-tipped drill bit, mounted in indium-filled Al holders, and gold-coated. Fluorine, Cl and  $\text{H}_2\text{O}$  were measured by SIMS using a Cameca 4f instrument at the Edinburgh Ion Microprobe Facility (EIMF), University of Edinburgh. A 5-nA primary beam of negative  $^{16}\text{O}$  ions accelerated to 14.5 kV was used. Pit diameter was ca. 15  $\mu\text{m}$ , depth of the analysis pits was <2  $\mu\text{m}$ . Total counting times were 30 s per isotope per analysis. Water and Cl were calibrated using an in-house basaltic glass standard (St81-A9; Lesne et al., 2011). Fluorine was calibrated using T1-G glass (Guggino and Hervig, 2010). Reproducibility for all elements, as determined by repeat measurements of glass standards, is better than 10% for all elements.

The use of glass standards may introduce a bias due to matrix effects. Therefore, amphibole standards of known  $\text{H}_2\text{O}$ , F and Cl contents were used to calibrate the matrix effects associated with Fe–Mg hydrous silicates. Correction factors of 1.4 for F and 1.9 for

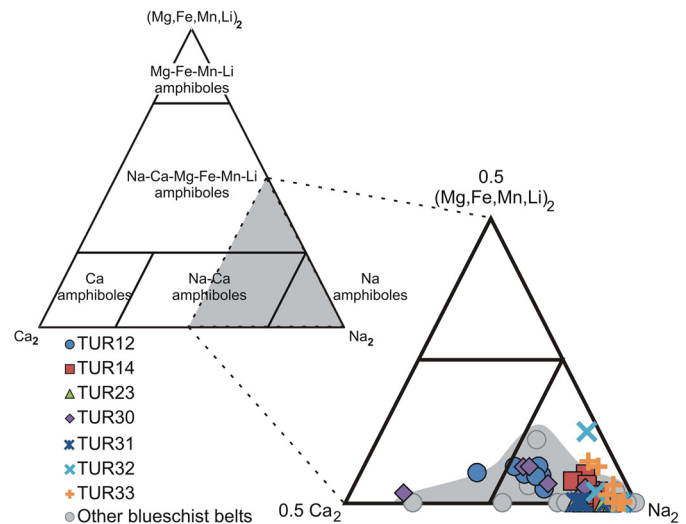


**Fig. 3.** Composition of amphiboles from lawsonite blueschists of the Tavasli Zone, northwestern Turkey. Classification based on B-site ( $B_2$ ) occupancy according to Leake et al. (2003). Modified from Hawthorne and Oberti (2006). For comparison, the composition of other blueschists in Turkey (e.g. Okay, 2002; Davis and Whitney, 2006), Greece (Schliestedt, 1986) and New Caledonia (Spandler et al., 2003) are plotted.

Cl were ascertained and applied to the analysis of Na-amphibole and phengite. No matrix-induced fractionation was observed for  $\text{H}_2\text{O}$ . Due to a lack of suitable standards for lawsonite, F and Cl contents of this mineral were calibrated using basaltic glass standards. Calibration curves can be found in supplementary material (Fig. S1).

## 5. Results

### 5.1. Bulk rock chemistry

Most samples have a basaltic chemical composition (44.4–52.1 wt%  $\text{SiO}_2$ ; Table S2 of supplementary files). Sample TUR31 has a slightly higher  $\text{SiO}_2$  content (58.0%), reflecting the abundant quartz veinlets in thin section. Although the overall composition is similar to that of tholeiitic basalts, the samples show some variations in major element abundance due to the coarse-grained nature of the samples. Samples have variable CaO (3.9–12.7 wt%) due to the presence of coarse-grained lawsonite, and moderate bulk-rock Mg# (0.49–0.74).  $\text{TiO}_2$  content of most samples (0.5–2.1 wt%) is consistent with a ridge basalt protolith rather than an arc basalt (White and Klein, 2014), and the presence of phengite in most samples corresponds to elevated  $\text{K}_2\text{O}$  (0.34–0.82 wt%) relative to typical N-MORB values. Two samples have very low bulk  $\text{K}_2\text{O}$  (<0.06%), and as a result contain only a very minor amount of phengite. High  $\text{P}_2\text{O}_5$  (up to 0.67 wt%) in most samples is consistent with the presence of apatite. Overall, major element data of the Tavasli Zone blueschists are consistent with their origin as basaltic rocks of the Izmir-Ankara Ocean.

### 5.2. Mineral chemistry

#### 5.2.1. Na-amphibole

All amphiboles are sodic following the classification of Leake et al. (2003), with Na dominating the B-site ( $\geq 1.50$  pfu; Table S3; Fig. 3). Other than minor K (<0.01 pfu), the A-site is vacant in all samples except for TUR31 which has high Na (<1.92 pfu). Most samples are characterized by high  $\text{Fe}^{3+}$  (0.242–1.80 pfu) in the C-site. Amphibole composition is similar to previous reports of blueschist amphiboles in this region (e.g. Okay, 2002; Davis and Whitney, 2006) and other HP belts (e.g. Schliestedt, 1986; Spandler et al., 2003; Fig. 3).

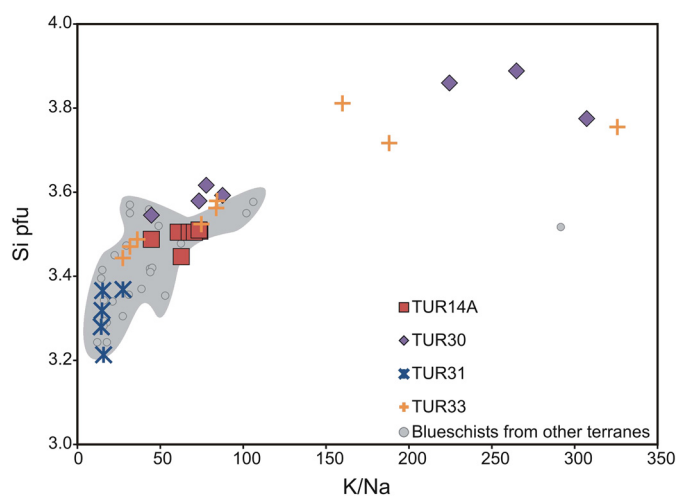


**Fig. 4.** Composition of phengite from lawsonite blueschists of the Tavsanli Zone, northwestern Turkey. Atomic ratios of K/Na increases with increasing Si atoms per formula unit (pfu). The compositions are similar to phengite in blueschists from other terranes, including New Caledonia (Spandler et al., 2003), the Catalina Schist, California (Bebout et al., 2007), Mariana forearc (Pabst et al., 2012), and the Sivrihisar Massif of the eastern Tavsanli Zone (Davis and Whitney, 2006).

### 5.2.2. Lawsonite

The lawsonite grains have near-ideal chemical composition with minimal variation among different grains, and among different samples (Table S4). Total Fe content is elevated, up to 2.3 wt%, compared to other lawsonites in blueschists worldwide (e.g. Spandler et al., 2003), but the values are similar to those of lawsonite of the Sivrihisar Massif in the eastern part of the Tavsanli Zone (Davis and Whitney, 2006).

### 5.2.3. Phengite

Phengite is common in TUR14, TUR30 and TUR33, and is a minor constituent of TUR23 and TUR31. In the latter, grains are small (<100 μm) and often intergrown with chlorite, making precise composition analysis difficult. Phengite composition in the Deliballar outcrop sample (TUR14) covers a narrow range (Si = 3.4–3.5 pfu; Table S5), similar to previous reports for white mica in other lawsonite blueschists in the world (e.g. Spandler et al., 2003; Davis and Whitney, 2006; Bebout et al., 2007). A wider spread in Si content (3.4–3.9 pfu) is observed for two samples from the Ketenlik outcrop (TUR30, TUR33). From the same outcrop, phengite in TUR31 has low Si (3.2–3.4 pfu) and K/Na (<30; Fig. 4), suggesting this sample may have re-equilibrated at low temperatures.

### 5.2.4. Apatite

Apatite in all samples contain high F (2.64–3.75 wt%), but low Cl (<0.06 wt%), classifying them as fluorapatites (Table S6; Fig. 5). In addition to CaO and P<sub>2</sub>O<sub>5</sub>, most samples contain minor amounts of MgO (<0.07 wt%), Na<sub>2</sub>O (<0.09 wt%), K<sub>2</sub>O (<0.15 wt%), SrO (<0.41 wt%), Ce<sub>2</sub>O<sub>3</sub> (<0.64 wt%), La<sub>2</sub>O<sub>3</sub> (<0.63 wt%), Al<sub>2</sub>O<sub>3</sub> (<0.1 wt%), SO<sub>3</sub> (<0.55 wt%), and As<sub>2</sub>O<sub>5</sub> (<0.17 wt%), along with variable FeO (<1.4 wt%) and SiO<sub>2</sub> (<2.3 wt%).

## 5.3. Halogens

### 5.3.1. Mineral fractions and bulk rock by pyrohydrolysis

Bulk rock Cl concentrations (8–22 ppm) are two orders of magnitude greater than those for Br (0.07–0.24 ppm) and I (0.13–0.52 ppm), with Br/Cl and I/Cl ratios covering a narrow range (0.006–0.019 and 0.011–0.024, respectively; Table S7). Fluorine is the most abundant halogen in all bulk samples, with concentrations ranging from 222 to 616 ppm and corresponding F/Cl ratios of 25.3 to 74.1.

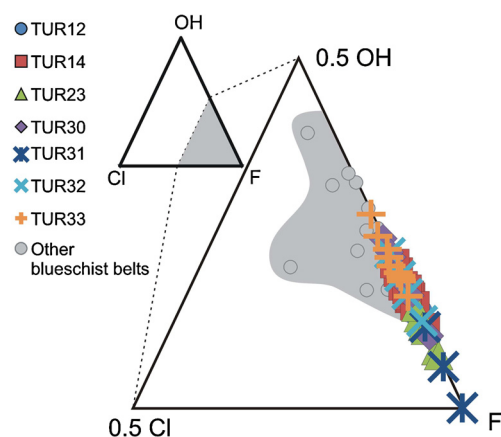


**Fig. 5.** Volatile contents (atomic proportion) in apatite from lawsonite blueschists of the Tavsanli Zone, northwestern Turkey. Hydroxyl component calculated by difference ( $X_{OH} = 1 - X_F - X_{Cl}$ ). There is overlap with apatites from other HP belts (e.g. Svensen et al., 2001; John et al., 2008), however in general the Tavsanli blueschists have higher F.

Mineral-rich fractions have a larger spread in halogen concentrations, particularly for F and Cl. Sodid amphibole-rich fractions show high F (198–608 ppm) compared to the heavier halogens (10–40 ppm Cl, 0.16–0.26 ppm Br, and 0.12–1.01 ppm I). Despite the wider spread in heavy halogen concentrations, their ratios fall within narrow ranges (0.005–0.016 Br/Cl, 0.011–0.025 I/Cl), but F/Cl ratios (7.9–38.4) do not. An even larger spread is observed for the halogen concentrations of lawsonite-rich fractions (120–955 ppm F, 8–56 ppm Cl, 0.14–0.47 ppm Br, and 0.14–1.37 ppm I), but the spread in Br/Cl and I/Cl ratios is narrow (0.008–0.021 and 0.018–0.024, respectively) compared to the spread in F/Cl ratios (8.8–37.2). The phengite-rich fraction has F/Cl, Br/Cl and I/Cl ratios of 34, 0.013 and 0.016, respectively.

Fluorine and Cl contents of bulk samples are broadly correlated with bulk K<sub>2</sub>O and P<sub>2</sub>O<sub>5</sub> (Fig. S2), providing evidence that phengite and apatite may influence the bulk halogen content of these blueschists.

### 5.3.2. Hydrous mineral concentrations by SIMS

Phengite and lawsonite contain higher F (372–572 ppm and 295–861 ppm, respectively) than Na-amphibole (84–390 ppm) (Table 2). Chlorine concentrations are lower than those of F for all three minerals and in all samples by an order of magnitude or more, agreeing with the results from bulk pyrohydrolysis extractions in this study. Phengite (21–77 ppm) and Na-amphibole (18–97 ppm) have similar concentrations, while lawsonite has lower Cl concentrations spanning a narrow range (20–46 ppm). Na-amphibole and lawsonite F/Cl ratios (0.97–21 and 11–36, respectively) cover a range of two orders of magnitude, similar to those of the corresponding extracted mineral fractions. Phengite F/Cl ratios also cover a range of two orders of magnitude (5–27), slightly lower than the ratio reported for the only phengite-rich mineral fraction.

### 5.3.3. Apatite concentrations by EPMA

Apatite contains higher F concentrations (up to 3.51 wt%; Table 2) than Na-amphibole, lawsonite and phengite, contributing up to 51% of total F in bulk samples. Chlorine concentrations in apatite are also elevated (up to 253 ppm) with respect to the other minerals, but to a lesser extent than F concentrations, as evidenced by apatite's higher F/Cl ratios (114–493).

### 5.3.4. Mineral partitioning

The distribution of halogens among Na-amphibole, phengite and lawsonite is varied across samples. In TUR30, F distributes

**Table 2**

Halogen concentrations in blueschist facies minerals from the Tavsanlı Zone, north-western Turkey. Na-amphibole, lawsonite and phengite results were determined by SIMS, and apatite by EPMA. Apatite concentrations are an average of 1–3 analyses/grain for 1–4 grains/sample, depending on grain size and abundance.

	H <sub>2</sub> O (wt%)	F (ppm)	Cl (ppm)	F/Cl
<b>Phengite</b>				
TUR14A	5.75	503	77	6.54
TUR30	5.77	572	21	26.9
TUR33	6.07	372	69	5.35
Average	5.87	482	56	12.9
<b>Na-amphibole</b>				
TUR12	2.15	218	46	4.79
TUR14A	2.17	335	97	3.47
TUR30	2.02	390	18	21.4
TUR32	2.09	256	46	5.60
TUR33	2.19	84	87	0.967
Average	2.12	257	59	7.25
<b>Lawsonite</b>				
TUR23	10.5	334	20	16.9
TUR30	10.1	383	33	11.8
TUR31	10.7	861	24	35.9
TUR32	10.4	295	27	10.8
TUR33	10.0	538	46	11.6
Average	10.3	482	30	17.4
<b>Apatite</b>				
TUR12		30600	nd	nd
TUR14A		30590	130	235
TUR23		32790	163	201
TUR30		29560	60	493
TUR31		35070	108	325
TUR32		31800	113	281
TUR33		28770	253	114
Average		31310	138	275

nd – not detected.

evenly between amphibole and lawsonite (distribution coefficient,  $D_{\text{Amp-Lws}}^{\text{F}} = 1.0$ ), and Cl concentrates in lawsonite ( $D_{\text{Amp-Lws}}^{\text{Cl}} = 0.56$ ). However, in TUR32 and TUR33, F partitions into lawsonite ( $D_{\text{Amp-Lws}}^{\text{F}} = 0.16$ – $0.87$ ) and Cl into amphibole ( $D_{\text{Amp-Lws}}^{\text{Cl}} = 1.67$ – $1.87$ ). Phengite/lawsonite distribution coefficients reveal F preferentially partitions into phengite ( $D_{\text{Ph-Lws}}^{\text{F}} = 1.5$ ) and Cl into lawsonite ( $D_{\text{Ph-Lws}}^{\text{Cl}} = 0.65$ ) for sample TUR30, but the reverse is observed ( $D_{\text{Ph-Lws}}^{\text{F}} = 0.69$ ,  $D_{\text{Ph-Lws}}^{\text{Cl}} = 1.5$ ) for TUR33. The phengite/amphibole distribution coefficients for Cl cover a small range around  $\sim 1$  (0.79–1.2, avg. 0.92), indicating equal partitioning in both minerals, whereas F preferentially concentrates in phengite ( $D_{\text{Ph-Amp}}^{\text{F}} = 1.5$ – $4.4$ , avg. 2.5) for all samples.

Fluorine concentrations in apatite are two to three orders of magnitude greater than in the hydrous minerals (Table 2). The partitioning of F between apatite and Na-amphibole is varied across all samples ( $D_{\text{Ap-Amp}}^{\text{F}} = 76$ – $343$ ), more so than the distribution between apatite and lawsonite ( $D_{\text{Ap-Lws}}^{\text{F}} = 41$ – $108$ ) or phengite ( $D_{\text{Ap-Ph}}^{\text{F}} = 52$ – $77$ ). The distribution of Cl between apatite and Na-amphibole ( $D_{\text{Ap-Amp}}^{\text{Cl}} = 1.3$ – $3.3$ ), lawsonite ( $D_{\text{Ap-Lws}}^{\text{Cl}} = 1.8$ – $8.2$ ), and phengite ( $D_{\text{Ap-Ph}}^{\text{Cl}} = 1.7$ – $3.6$ ) is similar for all three mineral pairings.

## 6. Discussion

### 6.1. Halogen concentrations in blueschists

Bulk rock halogen abundances were calculated based on the measured halogen concentrations of Na-amphibole, lawsonite, phengite and apatite along with their modal abundances in each sample. Calculated F and Cl values in bulk rock are generally in

good agreement with the measured bulk rock concentrations (Table S8). This verifies that there are no other major halogen-rich phases in the blueschist samples.

#### 6.1.1. Halogen uptake

Since the Tavsanlı zone blueschists are characterized by prograde mineral assemblages with very little retrogression (Table 1), halogens in these samples represent those deep in the subduction zone, as opposed to acquired during retrogression at shallow depths.

The presence of hydrous minerals and high Na in our samples are consistent with seafloor alteration prior to subduction, which should enrich Cl in basaltic rocks. However, the Cl content of these blueschists is much lower than that of the altered oceanic crust (e.g. 334 ppm; Sano et al., 2008), indicating that Cl may have been expelled before or during blueschist metamorphism.

Very few studies have been carried out on the abundance of Br and I in oceanic crust. Since amphibole is considered to be the major host of halogens in altered mafic rocks, the halogen concentrations of secondary amphibole from oceanic metagabbros (Kendrick et al., 2015) are used to approximate altered oceanic crust. The Br content of the metagabbros (0.46–1.98 ppm) is comparable to the range of Br in unaltered MORB (0.26–3.12 ppm; Kendrick et al., 2012), and up to an order of magnitude higher than Br concentrations in the Tavsanlı Zone blueschists. This may suggest that like Cl, Br is lost from the slab during subduction, however, elevated Br/Cl ratios with respect to unaltered and altered MORB (Fig. 7) may indicate preferential retention of Br in the down-going slab relative to Cl.

This study shows elevated abundances of I and F in bulk rock and mineral-rich fractions compared to the values in unaltered MORB (avg. 0.046 ppm I, Kendrick et al., 2012; avg. 147 ppm F, Le Roux et al., 2006) and altered oceanic crust (avg. 0.023 ppm I, Kendrick et al., 2015; avg. 216 ppm F, Straub and Layne, 2003). Seawater concentrations of F and I are too low to explain this enrichment. A plausible source of F and I are sediments on the sea floor or near subduction zones (e.g. John et al., 2011). High F values are reported in pelagic clays (up to 1300 ppm; Li, 1982) and organic-rich sediments, in particular, contain high concentrations of I (e.g. Muramatsu et al., 2007). Following fluid circulation through overlying sediments near subduction zones, it is likely that the oceanic crust becomes enriched in F and I on the sea floor prior to subduction, or along bending-related extensional faults at the outer rise. In addition, a large supply of I-rich shallow water sediments would have been available given the close proximity of continents to this particular subduction zone.

#### 6.1.2. Halogen fractionation

A positive correlation between Cl, Br and I in mineral fractions suggests an overall similar behaviour in subduction zones (Figs. 6a, b). Conversely, F concentrations do not correlate well with the heavier halogens (Fig. 6c). This difference in behaviour of halogens is attributed to the enhanced reactivity of F due to its smaller size and higher electronegativity. Of the four halogens, the ionic radius (1.33 Å) of F is most similar to that of OH<sup>−</sup> (1.35 Å), making it most compatible for substitution in hydrous minerals. An additional mechanism for the incorporation of F into silicate minerals is the coupled substitution of Al<sup>3+</sup> and F<sup>−</sup> with Si<sup>4+</sup> and O<sup>2−</sup> (1.21 Å), as previously suggested to explain F uptake in pyroxenes (Mosenfelder and Rossman, 2013). The elevated I/Cl, Br/Cl and F/Cl ratios of our samples relative to altered oceanic crust (Fig. 7), suggest either I, Br and F are enriched in the crust prior to subduction, or these halogens are preferentially retained relative to Cl during subduction-related metamorphism.

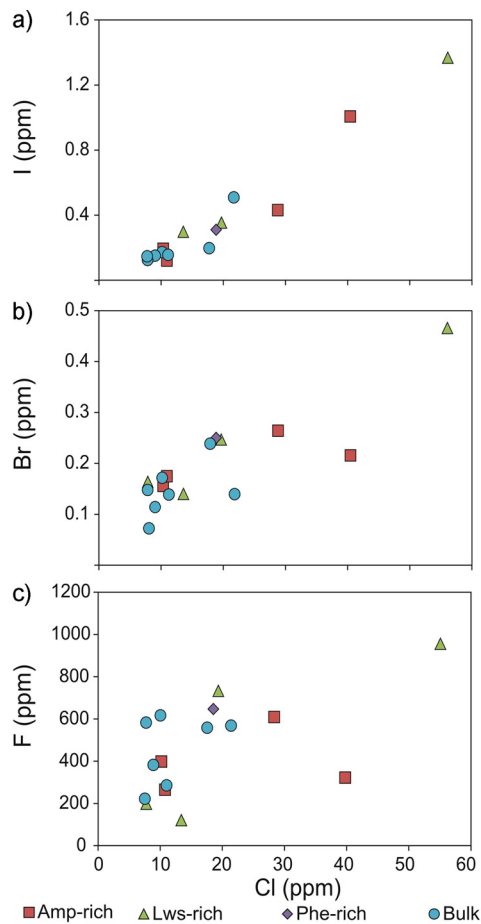


**Fig. 6.** Halogen content of bulk samples and mineral separates for lawsonite blueschists of the Tavsanli Zone, northwestern Turkey. Chlorine is plotted against (a) I, (b) Br and (c) F. There is a positive correlation between Cl, Br and I, but not F.

## 6.2. Halogen partitioning between hydrous minerals

### 6.2.1. Chlorine

Chlorine preferentially partitions into phengite and Na-amphibole, with average concentrations for each mineral in all samples of 59 ppm for Na-amphibole, 56 ppm for phengite and 27 ppm for lawsonite (Table 2). The low Cl content of lawsonite may be related to structural differences among the three minerals. Micas and amphiboles have appreciably more  $M^{2+}$  cations in their octahedral sites than lawsonite, which minimizes distortion of their hydroxyl sites and allows for greater substitution of  $Cl^-$  in the  $OH^-$  site (Volfinger et al., 1985). Furthermore, hydrogen bonding may also affect halogen uptake. Amphibole and phengitic muscovite have weak hydrogen bonding (Catlow and Wright, 1999; Gatta et al., 2011), but lawsonite contains multiple hydrogen bonds (Libowitzky and Rossman, 1996). Therefore, hydroxyl substitution may be less energetically favourable in lawsonite given the additional energy requirements to overcome these bonds.

### 6.2.2. Fluorine

In situ measurements reveal F preferentially concentrates in phengite (avg. 482 ppm) and lawsonite (avg. 482 ppm) over Na-amphibole (257 ppm). Fluorine may be more readily retained by phengite and lawsonite due to an increase in the electrostatic attraction between F and interlayer  $K^+$  in phengite and A-site  $Ca^{2+}$  in lawsonite. When  $F^-$  substitutes for  $OH^-$ , the reduced distance between the halogen and interlayer/cavity cations allows for a greater attraction between them. The Na-amphiboles, on the other hand,

have vacancy in the A-site, and thus may not as readily retain F. Our results are in agreement with data from other eclogites showing higher F in phengite over co-existing amphiboles (e.g. Svensen et al., 2001).

### 6.2.3. Bromine and iodine

Partitioning of Br and I between co-existing minerals is evaluated from pyrohydrolysis extractions of amphibole- and lawsonite-rich fractions. Bromine concentrations appear uniform between both mineral phases in all samples, except for TUR33 in which the lawsonite concentrate has two times more Br. Iodine seems to preferentially partition into lawsonite, as observed by elevated concentrations in the lawsonite-rich fractions of TUR 30, 32 and 33. In addition to substitution for  $OH^-$  groups, large cavities containing  $H_2O$  and  $Ca^+$  in lawsonite's structure may accommodate I ions.

## 6.3. Halogens in apatite

Apatite preferentially incorporates F from fluids (Spear and Pyle, 2002), and the small F ion can easily fit in the columnar anion site, coplanar with the M2 cations. In contrast, Cl and OH ions are too large, and are displaced above or below the cation plane. With increasing pressure, the incorporation of small F is favoured. Since F is an essential component of fluorapatites, it is preferentially concentrated in apatite over other minerals, such as amphibole, lawsonite and phengite. The halogen abundance of apatite in our samples is similar to metamorphic apatite from Norwegian eclogites (Svensen et al., 2001). Measured F contents in phengite in our samples are similar, but those in Na-amphibole and lawsonite are higher than those in blueschist facies metagabbros reported by Debret et al. (2016). Furthermore, their estimated bulk F contents based on concentrations in these minerals and their modal abundances are much lower than our measured values. The difference may be related to apatite since it is the major mineral phase hosting F in our samples, but is not considered in their calculations as their samples may contain low P.

## 6.4. Implications for halogen recycling

Low Cl concentrations recorded for all hydrous minerals in these samples imply that Cl is expelled at much shallower depths in the subduction zone. This is in good agreement with previous estimates that as much as 75% of the subducted Cl in rocks and pore fluids may be released from the accretionary prism at slab depth <15 km (Jarrard, 2003). Metamorphism before or during the blueschist facies may also contribute to Cl loss from the subducting slab before 80 km depth. This proposed interpretation is supported by the broad correlation between bulk rock Cl and As concentrations (0.5–2.2 ppm) (Fig. S3). Since As is lost early from subducting slabs (<35 km depth; Hattori et al., 2005), the evidence supports Cl loss in addition to other fluid-mobile elements during shallow subduction. Similarly low concentrations of Cl have been reported for bulk rock blueschists (60–300 ppm) and eclogites (30–60 ppm) from the island of Syros, Greece (Marschall et al., 2009).

In contrast, elevated F concentrations in these blueschists suggest F is retained during subduction to at least 80 km depth. A positive correlation between F and Be in our bulk rocks (Fig. S3) supports this interpretation, since Be exhibits conservative behaviour during subduction-related dehydration reactions (Marschall et al., 2007).

Na-amphibole decomposition at <90 km depth (associated with the blueschist–eclogite transition) has been proposed to contribute to partial melting for arc magmatism (Peacock, 1993). However, the F/Cl ratios for Na-amphibole in these blueschists are higher than those reported for volcanic arc outputs and back-arc basin

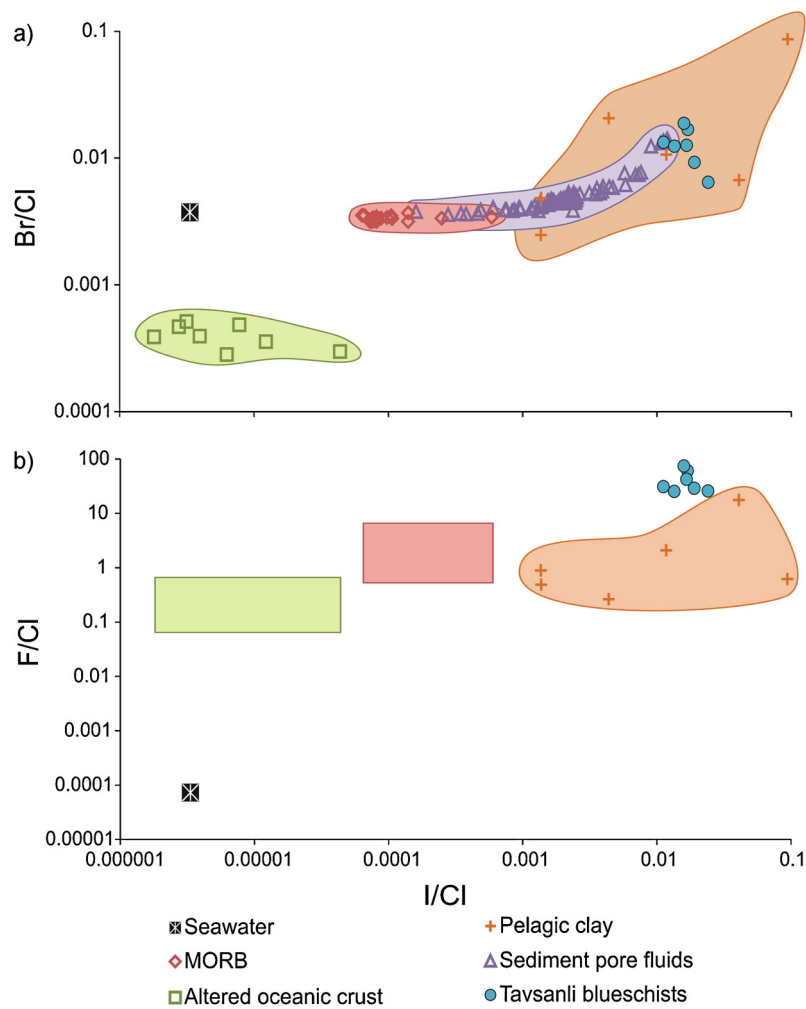


**Fig. 7.** Compilation of halogen ratios in unaltered and altered oceanic crust, sedimentary marine reservoirs and Tavsanlı Zone blueschist bulk rocks. (a) Given the scarcity of bulk rock data for Br and I in altered oceanic crust, Br/Cl and I/Cl of secondary amphiboles in oceanic metagabbros (Kendrick et al., 2015) are used as a proxy for altered oceanic crust. The low Br/Cl ratios of the altered oceanic crust relative to unaltered MORB and seawater (Li, 1982) suggest Cl is preferentially incorporated into amphibole over Br during hydrothermal alteration. Br/Cl and I/Cl ranges for MORB (Kendrick et al., 2012) overlap with the lower range of pore fluids of marine sediments (Muramatsu et al., 2007). Pore fluid data extends to higher values, overlapping with incoming plate sediments (John et al., 2011), and the Tavsanlı zone blueschists analyzed in this study. (b) The F/Cl range for altered oceanic crust (Magenheim et al., 1995) is lower than that of unaltered MORB (Le Roux et al., 2006), but significantly elevated relative to seawater (Li, 1982). F/Cl values of the Tavsanlı blueschists are higher than MORB values, and overlap with the upper range of incoming plate sediments.

basalts (Fig. 8), suggesting amphibole dehydration may not be the dominant source for these halogen signatures. Given the relatively shallow depth of dehydration, Na-amphibole is likely not relevant for the transfer of halogens to the deeper mantle. However, F in the amphibole structure may widen its stability to higher pressures and temperatures, allowing F-rich Na-amphibole to remain stable under eclogite facies conditions (Holloway and Ford, 1975), and carry F to greater depths.

The high F contents of lawsonite and phengite in this study are of particular interest given the wide stability of these minerals in cool subduction zones. Lawsonite is stable to 80–90 kbar, and phengite to 100 kbar, at 900 °C (Schmidt and Poli, 1998). Once they decompose, the resulting fluids would have high F/Cl ratios. It is interesting to note that these ratios are comparable to melt formed at deep levels, including ocean island basalts (e.g. Hauri, 2002; Kendrick et al., 2015), and kimberlites (e.g. Paul et al., 1976) (Fig. 8), suggesting the importance of these minerals for the transfer of F to the deep mantle.

Despite not contributing to the water budget of subducting slabs, apatite is likely an important repository of halogens during HP metamorphism, transporting F (and some Cl) beyond subarc depths. Upon apatite breakdown at ~200 km, halogens in apatite

may be released to the overlying mantle, or possibly incorporated into stable hydrous silicates such as phengite and lawsonite (Konzett and Frost, 2009).

Chlorite (12 wt% H<sub>2</sub>O) is present in variable abundance in all samples, and the texture and occurrence suggest it is a prograde product. Chlorite stability is primarily temperature dependent, and in cold subduction zones it may remain stable to 40+ kbar (~100+ km; Mookherjee and Mainprice, 2014). Although we did not determine halogen contents in chlorite due to its intergrowth with other minerals, the bulk rock data for chlorite-rich TUR31 (582 ppm F, 8 ppm Cl) suggest chlorite likely contains F and Cl concentrations similar to the other hydrous minerals, and there is little partitioning of F and Cl between chlorite and other minerals.

Low Cl and high F content in the Tavsanlı Zone blueschists support previously proposed interpretation based on the halogen content of arc magmas that Cl is effectively liberated during subduction at shallow depths, whereas F is largely retained in the down-going slab beyond arc front depths (Straub and Layne, 2003). Liberation of Cl during early subduction is also documented by expulsion of saline fluids from accretionary prisms (e.g. Godon et al., 2004). High I/Cl ratios of bulk samples and mineral separates suggest I may be fractionated from Cl during subduction, and like F,



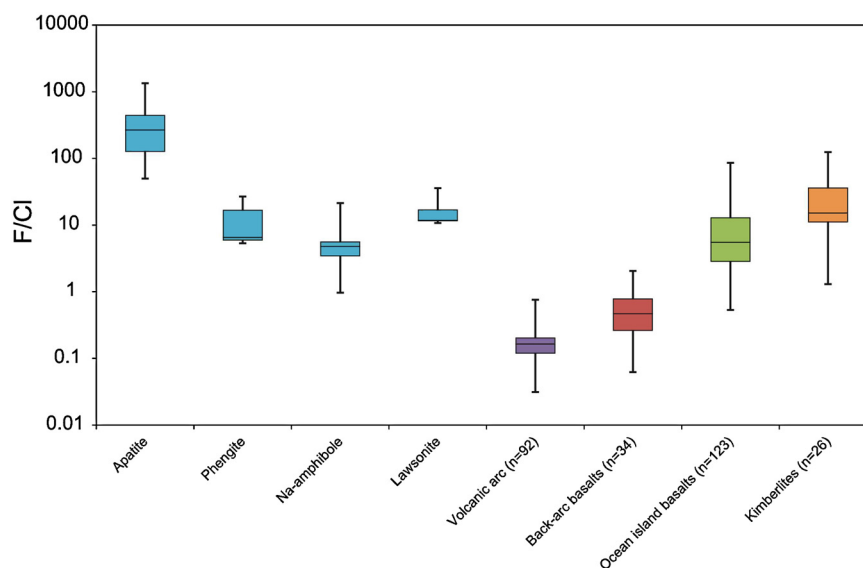


**Fig. 8.** Box-and-whisker plot displaying the F/Cl ratios of apatite, Na-amphibole, lawsonite and phengite from the Tavsanli Zone blueschists, northwestern Turkey. For comparison, F/Cl ratios for various magmas have been added. High F/Cl ratios of lawsonite and phengite suggest these minerals may provide a means for transporting F to the deep upper mantle, supplying magmas of deeper origin such as ocean island basalts (e.g. Hawaiian melt inclusions, Hauri, 2002; Samoa glasses, Kendrick et al., 2015) and kimberlites (e.g. bulk rock from Greenland, South Africa and India, Paul et al., 1976). Volcanic arc data are from Lesser Antilles melt inclusions (Heath et al., 1998), Central American Arc pyroclastic rocks (John et al., 2011), and Izu Arc glasses and fallout tephra (Straub and Layne, 2003). Back-arc basalt data are bulk rock data from the Lau Basin (Bézos et al., 2009).

incorporated into hydrous minerals. Bromine may also be fractionated from Cl based on slightly elevated Br/Cl ratios, but to a much lesser extent than F or I. Chlorine, and most Br, is likely released before or during blueschist metamorphism, whereas F is retained in phengite, lawsonite and apatite at blueschist depth. When apatite eventually breaks down at ~200 km, F may be re-distributed to phengite and lawsonite, whereas minor Cl in apatite is most likely released to the overlying mantle wedge. Finally, at ~280–300 km in cold subduction zones, lawsonite and phengite decompose, releasing F to the deeper upper mantle.

### 6.5. Conclusions

Hydrous blueschist minerals of the Tavsanli Zone contain high F and low Cl concentrations, suggesting F is preferentially retained, whereas Cl is lost at shallow depths (<80 km) in subduction zones. A positive correlation between Cl, Br and I contents of the pyrohydrolysis extracts suggests Br and I may behave similarly to Cl in subduction zones, although high I/Cl and slightly high Br/Cl ratios relative to MORB indicate some fractionation of I and Br from Cl during subduction and blueschist facies metamorphism.

Chlorine partitioning among the four analysed minerals follows apatite > phengite ≈ Na-amphibole > lawsonite, and F partitioning follows apatite ≫ phengite ≈ lawsonite > Na-amphibole. The halogens preferentially reside in apatite because they are accommodated in the M2 site. The eventual decomposition of apatite at ~200 km may lead to a redistribution of F into lawsonite and phengite. The accommodation of F in lawsonite and phengite suggests F may be transported by these minerals to a depth of 280–300 km in cold subduction zones, and may contribute to the high F content observed in deep mantle magmas, such as ocean island basalts and kimberlites.

### Acknowledgements

This paper is part of the first author's PhD thesis research project at the University of Ottawa. We thank Paul Middlestead for pyrohydrolysis set-up assistance, Nimal De Silva for ICP mass spectrometry analyses, Ping Zhang for ion chromatography analyses,

Glenn Poirier for electron microprobe assistance, George Mrazek for preparation of polished thin sections, John Hopkins for customized glassware, Jack Cornett for consultation on pyrohydrolysis method development, and Tom Pestaj and Bill Davis of the Geological Survey of Canada (GSC) for thin section coring assistance. We also thank editor Bernard Marty for his handling of this manuscript, and are grateful for the constructive comments provided by Mark Kendrick and an anonymous reviewer for the improvement of this article. The research was supported by an NSERC Discovery Grant provided to Keiko Hattori.

### Appendix A. Pyrohydrolysis method for halogen extraction

A 0.5 g weight of finely ground sample was combined in a silica boat with an equal weight of reagent grade V<sub>2</sub>O<sub>5</sub> (Elemental Microanalysis Ltd) previously heated to 325 °C for 24 h. A wet oxygen gas flow of 0.8 Lmin<sup>-1</sup> was created using an Erlenmeyer flask of water on low heat connected to a tank of UHP oxygen gas. The main silica tube was housed in a Lindberg Blue M tube furnace set at an initial temperature of 500 °C. A glass rod was used to insert a silica wool plug into the main tube and position it just beyond the wall of the furnace. The purpose of plug was to prevent solid material from entering the trap and clogging the frit. The sample was slowly introduced to the main tube and positioned directly in the middle of the furnace. Once the system was reconnected, the furnace temperature was increased to 1100 °C for 15 min. The temperature on the output end of the main tube beyond the furnace was maintained at 120 °C+ with heating tape to prevent condensation. The evolved gas was passed through a frit inside the trap to maximize surface area contact with the 7 mL of 25 mM NaOH trap solution (prepared from extra pure N<sub>2</sub>-flushed NaOH pellets from Acros Organics). The collection vessel was submerged in an ice bath during collection to promote condensation of the halogens in solution. After 15 min the furnace temperature was reduced to 500 °C before expelling the sample and quartz wool from the main tube. The system was purged with oxygen for 10–15 min, fresh quartz wool and the next sample were inserted, and a clean collection vessel was connected to the trap. All glassware was cleaned with deionized water after every two to three runs (i.e. duplicates

or triplicates of one sample). Collected solutions were diluted 5x for ICP-MS analysis, and 1% HNO<sub>3</sub> was added to stabilize anions in solution. Dilution was not necessary for IC analysis.

## Appendix B. Supplementary material

Supplementary material related to this article can be found online at <http://dx.doi.org/10.1016/j.epsl.2016.02.054>.

## References

- Bebout, G.E., Bebout, A.E., Graham, C.M., 2007. Cycling of B, Li, and LILE (K, Cs, Rb, Ba, Sr) into subduction zones: SIMS evidence from micas in high-*P/T* metasedimentary rocks. *Chem. Geol.* 239 (3), 284–304.
- Bézos, A., Escrig, S., Langmuir, C.H., Michael, P.J., Asimow, P.D., 2009. Origins of chemical diversity of back-arc basin basalts: a segment scale study of the Eastern Lau Spreading Center. *J. Geophys. Res., Solid Earth* (1978–2012) 114 (B6).
- Catlow, C.R.A., Wright, K. (Eds.), 1999. *Microscopic Properties and Processes in Minerals*, vol. 543. Springer, p. 495.
- Davis, P.B., Whitney, D.L., 2006. Petrogenesis of lawsonite and epidote eclogite and blueschist, Sivrihisar Massif, Turkey. *J. Metamorph. Geol.* 24 (9), 823–849.
- Debret, B., Koga, K.T., Cattani, F., Nicollet, C., Van den Bleeken, G., Schwartz, S., 2016. Volatile (Li, B, F and Cl) mobility during amphibole breakdown in subduction zones. *Lithos* 244, 165–181.
- Gatta, G.D., McIntyre, G.J., Sassi, R., Rotiroli, N., Pavese, A., 2011. Hydrogen-bond and cation partitioning in muscovite: a single-crystal neutron-diffraction study at 295 and 20 K. *Am. Mineral.* 96 (1), 34–41.
- Godon, A., Jendrzewski, N., Castrec-Rouelle, M., Dia, A., Pineau, F., Boulègue, J., Javoy, M., 2004. Origin and evolution of fluids from mud volcanoes in the Barbados accretionary complex. *Geochim. Cosmochim. Acta* 68 (9), 2153–2165.
- Goldoff, B., Webster, J.D., Harlov, D.E., 2012. Characterization of fluor-chlorapatites by electron probe microanalysis with a focus on time-dependent intensity variation of halogens. *Am. Mineral.* 97 (7), 1103–1115.
- Guggino, S.N., Hervig, R.L., 2010. Determination of fluorine in fourteen microanalytical geologic reference materials using SIMS, EPMA, and proton induced gamma ray emission (PIGE) analysis. In: *AGU Fall Meeting Abstracts*, Vol. 1. 2209.
- Hattori, K., Takahashi, Y., Guillot, S., Johanson, B., 2005. Occurrence of arsenic (V) in forearc mantle serpentinites based on X-ray absorption spectroscopy study. *Geochim. Cosmochim. Acta* 69 (23), 5585–5596.
- Hauri, E., 2002. SIMS analysis of volatiles in silicate glasses, 2: isotopes and abundances in Hawaiian melt inclusions. *Chem. Geol.* 183 (1), 115–141.
- Hawthorne, F.C., Oberti, R., 2006. On the classification of amphiboles. *Can. Mineral.* 44 (1), 1–21.
- Heath, E., Macdonald, R., Belkin, H., Hawkesworth, C., Sigurdsson, H., 1998. Magmatogenesis at Soufriere Volcano, St Vincent, Lesser Antilles Arc. *J. Petrol.* 39 (10), 1721–1764.
- Holloway, J.R., Ford, C.E., 1975. Fluid-absent melting of the fluoro-hydroxy amphibole pargasite to 35 kilobars. *Earth Planet. Sci. Lett.* 25 (1), 44–48.
- Jarrard, R.D., 2003. Subduction fluxes of water, carbon dioxide, chlorine, and potassium. *Geochim. Geophys. Geosyst.* 4 (5).
- John, T., Klemm, R., Gao, J., Garbe-Schönberg, C.D., 2008. Trace-element mobilization in slabs due to non steady-state fluid–rock interaction: constraints from an eclogite-facies transport vein in blueschist (Tianshan, China). *Lithos* 103 (1), 1–24.
- John, T., Scambelluri, M., Frische, M., Barnes, J.D., Bach, W., 2011. Dehydration of subducting serpentinite: implications for halogen mobility in subduction zones and the deep halogen cycle. *Earth Planet. Sci. Lett.* 308 (1), 65–76.
- Kendrick, M.A., Honda, M., Pettke, T., Scambelluri, M., Phillips, D., Giuliani, A., 2013. Subduction zone fluxes of halogens and noble gases in seafloor and forearc serpentinites. *Earth Planet. Sci. Lett.* 365, 86–96.
- Kendrick, M.A., Jackson, M.G., Hauri, E.H., Phillips, D., 2015. The halogen (F, Cl, Br, I) and H<sub>2</sub>O systematics of Samoan lavas: assimilated-seawater, EM2 and high-<sup>3</sup>He/<sup>4</sup>He components. *Earth Planet. Sci. Lett.* 410, 197–209.
- Kendrick, M.A., Kamenetsky, V.S., Phillips, D., Honda, M., 2012. Halogen systematics (Cl, Br, I) in mid-ocean ridge basalts: a Macquarie Island case study. *Geochim. Cosmochim. Acta* 81, 82–93.
- Konzett, J., Frost, D.J., 2009. The high *P-T* stability of hydroxyl-apatite in natural and simplified MORB—an experimental study to 15 GPa with implications for transport and storage of phosphorus and halogens in subduction zones. *J. Petrol.* 50 (11), 2043–2062.
- Le Roux, P.J., Shirey, S.B., Hauri, E.H., Perfit, M.R., Bender, J.F., 2006. The effects of variable sources, processes and contaminants on the composition of northern EPR MORB (8–10°N and 12–14°N): evidence from volatiles (H<sub>2</sub>O, CO<sub>2</sub>, S) and halogens (F, Cl). *Earth Planet. Sci. Lett.* 251 (3), 209–231.
- Leake, B.E., Woolley, A.R., Birch, W.D., Burke, E.A., Ferraris, G., Grice, J.D., Whittaker, E.J., 2003. Nomenclature of amphiboles: additions and revisions to the International Mineralogical Association's 1997 recommendations. *Can. Mineral.* 41 (6), 1355–1362.
- Lesne, P., Kohn, S.C., Blundy, J., Witham, F., Botcharnikov, R.E., Behrens, H., 2011. Experimental simulation of closed-system degassing in the system basalt–H<sub>2</sub>O–CO<sub>2</sub>–S–Cl. *J. Petrol.* 52 (9), 1737–1762.
- Li, Y.H., 1982. A brief discussion on the mean oceanic residence time of elements. *Geochim. Cosmochim. Acta* 46 (12), 2671–2675.
- Libowitzky, E., Rossman, G.R., 1996. FTIR spectroscopy of lawsonite between 82 and 325 K. *Am. Mineral.* 81, 1080–1091.
- Lyubetskaya, T., Korenaga, J., 2007. Chemical composition of Earth's primitive mantle and its variance: 1. Method and results. *J. Geophys. Res., Solid Earth* (1978–2012) 112 (B3).
- Magenheim, A.J., Spivack, A.J., Michael, P.J., Gieskes, J.M., 1995. Chlorine stable isotope composition of the oceanic crust: implications for Earth's distribution of chlorine. *Earth Planet. Sci. Lett.* 131 (3), 427–432.
- Marschall, H.R., Altherr, R., Gmeling, K., Kasztovszky, Z., 2009. Lithium, boron and chlorine as tracers for metasomatism in high-pressure metamorphic rocks: a case study from Syros (Greece). *Mineral. Petrol.* 95 (3–4), 291–302.
- Marschall, H.R., Altherr, R., Rüpke, L., 2007. Squeezing out the slab—modelling the release of Li, Be and B during progressive high-pressure metamorphism. *Chem. Geol.* 239 (3), 323–335.
- Mookherjee, M., Mainprice, D., 2014. Unusually large shear wave anisotropy for chlorite in subduction zone settings. *Geophys. Res. Lett.* 41 (5), 1506–1513.
- Mosenfelder, J.L., Rossman, G.R., 2013. Analysis of hydrogen and fluorine in pyroxenes: II. Clinopyroxene. *Am. Mineral.* 98 (5–6), 1042–1054.
- Muramatsu, Y., Doi, T., Tomaru, H., Fehn, U., Takeuchi, R., Matsumoto, R., 2007. Halogen concentrations in pore waters and sediments of the Nankai Trough, Japan: implications for the origin of gas hydrates. *Appl. Geochem.* 22 (3), 534–556.
- Okay, A.I., 1980. Mineralogy, petrology, and phase relations of glaucophane-lawsonite zone blueschists from the Tavşanlı Region, Northwest Turkey. *Contrib. Mineral. Petrol.* 72 (3), 243–255.
- Okay, A.I., 2002. Jadeite–chloritoid–glaucophane–lawsonite blueschists in northwest Turkey: unusually high *P/T* ratios in continental crust. *J. Metamorph. Geol.* 20 (8), 757–768.
- Okay, A.I., Whitney, D.L., 2010. Blueschists, eclogites, ophiolites and suture zones in northwest Turkey: a review and a field excursion guide. *Ophiolite* 35 (2), 131–172.
- Pabst, S., Zack, T., Savov, I.P., Ludwig, T., Rost, D., Tonarini, S., Vicenzi, E.P., 2012. The fate of subducted oceanic slabs in the shallow mantle: insights from boron isotopes and light element composition of metasomatized blueschists from the Mariana forearc. *Lithos* 132, 162–179.
- Paul, D.K., Buckley, F., Nixon, P.H., 1976. Fluorine and chlorine geochemistry of kimberlites. *Chem. Geol.* 17, 125–133.
- Peacock, S.M., 1993. The importance of blueschist → eclogite dehydration reactions in subducting oceanic crust. *Geol. Soc. Am. Bull.* 105 (5), 684–694.
- Sano, T., Miyoshi, M., Ingle, S., Banerjee, N.R., Ishimoto, M., Fukuoka, T., 2008. Boron and chlorine contents of upper oceanic crust: basement samples from IODP Hole 1256D. *Geochim. Geophys. Geosyst.* 9 (12).
- Scambelluri, M., Müntener, O., Ottolini, L., Pettke, T., Vannucci, R., 2004. The fate of B, Cl and Li in the subducted oceanic mantle and in the antigorite breakdown fluids. *Earth Planet. Sci. Lett.* 222 (1), 217–234.
- Schliestedt, M., 1986. Eclogite–blueschist relationships as evidenced by mineral equilibria in the high-pressure metabasic rocks of Sifnos (Cycladic Islands), Greece. *J. Petrol.* 27 (6), 1437–1459.
- Schmidt, M.W., Poli, S., 1998. Experimentally based water budgets for dehydrating slabs and consequences for arc magma generation. *Earth Planet. Sci. Lett.* 163 (1), 361–379.
- Sherlock, S., Kelley, S., Inger, S., Harris, N., Okay, A., 1999. <sup>40</sup>Ar–<sup>39</sup>Ar and Rb–Sr geochronology of high-pressure metamorphism and exhumation history of the Tavşanlı Zone, NW Turkey. *Contrib. Mineral. Petrol.* 137 (1–2), 46–58.
- Spandler, C., Hermann, J., Arculus, R., Mavrogenes, J., 2003. Redistribution of trace elements during prograde metamorphism from lawsonite blueschist to eclogite facies; implications for deep subduction-zone processes. *Contrib. Mineral. Petrol.* 146 (2), 205–222.
- Spear, F.S., Pyle, J.M., 2002. Apatite, monazite, and xenotime in metamorphic rocks. *Rev. Mineral. Geochem.* 48 (1), 293–335.
- Straub, S.M., Layne, G.D., 2003. The systematics of chlorine, fluorine, and water in Izu arc front volcanic rocks: implications for volatile recycling in subduction zones. *Geochim. Cosmochim. Acta* 67 (21), 4179–4203.
- Svensen, H., Jamtveit, B., Banks, D.A., Austrheim, H., 2001. Halogen contents of eclogite facies fluid inclusions and minerals: caledonides, western Norway. *J. Metamorph. Geol.* 19 (2), 165–178.
- Symonds, R.B., Rose, W.I., Bluth, G.J.S., Gerlach, T.M., 1994. Volcanic gas studies – methods, results, and applications. *Rev. Miner.* 30, 1–66.
- Volfinger, M., Robert, J.L., Vielzeuf, D., Neiva, A.M.R., 1985. Structural control of the chlorine content of OH-bearing silicates (micas and amphiboles). *Geochim. Cosmochim. Acta* 49 (1), 37–48.
- White, W.M., Klein, E.M., 2014. Composition of the oceanic crust. In: *Treatise on Geochemistry*, vol. 4, pp. 457–496.